A SIMPLE METHOD OF CORTICAL BONE THICKNESS EVALUATION BASED ON RADIOGRAPHIC IMAGES FOR OSTEOPOROSIS INVESTIGATION

Przemysław Maćkowiak, Ryszard Stasiński

Department of Electronics and Telecommunications,Poznań University of Technology, Polanka 3, Poznań, Poland

Tomasz Kulczyk

Department of Biomaterials and Experimental Dentistry, Poznań University of Medical Sciences, Poland

Keywords: Osteoporosis population screening, Dental panoramic radiographs, Automatic bone borders extraction.

Abstract: In the paper a method of automatic extraction of cortical bone based on dental panoramic radiographs is described. The method is intended for use as the first contact tool in osteoporosis population screening. Its components have very low computational complexity, and can be found in every image processing software package. The upper and lower boundaries of mandibular cortical bone have been determined in a series of panoramic images, and results have been evaluated by a radiologist. The technique works either very precisely, or clearly wrong (for heavily cluttered images), which proves its usefulness for an untrained user.

1 INTRODUCTION

Osteoporosis is a disease primarily affecting older people, especially women aged over 60, and which may lead to wrist, hip and vertebra fractures (Torsoni et al., 2006). The modern gold standard for evaluating osteoporosis is a BMD (Bone Mineral Density) examination of the lumbar spine or/and femoral neck. Currently access to a BMD examination is limited as it is not possible to carry out screening of all women over 65.

An alternative population screening test may be based on the evaluation of certain parameters of dental panoramic radiographs (Horner et al., 2002). Dental panoramic images show the facial parts of the skull with the upper and lower jaw and some neighbouring structures. A particularly interesting structure visible in a panoramic image is the cortical bone of the lower border of mandible in the vicinity of the mental foramen (Figure 1). Its parameters, e.g. the width of the cortical bone and distance from the lower border of the mandible to the mental foramen can be measured as well as some characteristic morphological features of the bone. If CW is below 3mm, an individual should be referred for the further osteoporosis investigation (Horner et al., 2002).
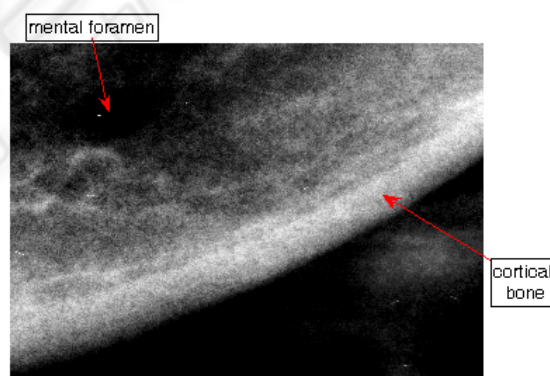

Figure 1: Portion of a dental panoramic radiograph showing the cortical bone and the mental foramen.

Analysis of morphological structures, in conjunction with the results of measurements such as PMI (Panoramic Mandibular Index), have been correlated with data from a BMD test to investigate any relationship between them. Some authors believe that analysis of a panoramic image can result in a dentist advising his patient to have a BMD test, "because from your dental panoramic image it looks as though you are in danger of osteoporosis" (Devlin et al., 2007). The advantages of such a "screening test" are both economic and safe, since the

panoramic image has already been taken for other purposes and the patient is not subject to additional radiation. Such a test should be automated, as evaluations done by general dental practitioners may differ importantly from those given by radiologists (Devlin et al., 2001).

Currently it exists only few works on automatic analysis of panoramic images for osteoporosis examination, and the based on active contours (snakes) method from paper (Devlin et al., 2007) requires specialised software. This article presents a computer algorithm consisting of simple and readibly available components, which seems to provide reliable measurements of the cortical bone.

The article is divided as follows. Chapter two describes the research material. Third chapter is the algorithm description. The fourth and the fifth chapter are the discussion and the results. The last ones are the conclusions and the literature.
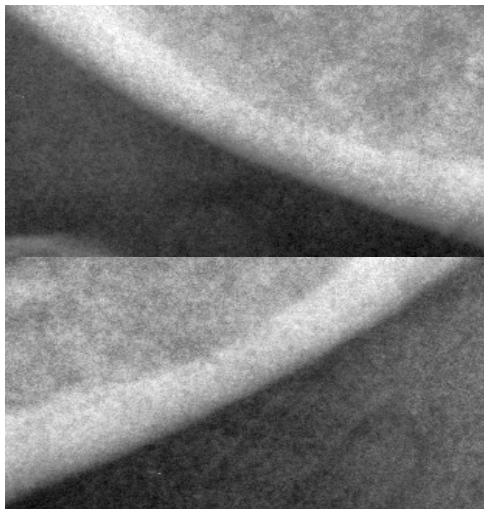

Figure 2: The region of interests for the right and left sides of a panoramic radiograph at the mandible.

2 RESEARCH MATERIAL

40 digital dental panoramic images have been taken using the CRANEX TOME dental panoramic unit and a DIGORA PCT PSP DIGITAL SCANNER. Images of 3258x1764 resolution have been provided by the Section of Dental Radiology in the Department of Biomaterials and Experimental Dentistry, Poznań University of Medical Sciences. Two small parts of the image from the left and right sides were cut off by the radiologist to create regions of interest (ROI) for further analysis. Each ROI has had a rectangular shape and has contained the region

extending from edge of mental foramen down to and below the lower edge of cortical bone, as illustrated in Figure 2. The size of the ROI may vary but must include the region around the mental foramen and extend below the lower border of mandible.

3 ALGORITHM DESCRIPTION

The goal is to determine the upper and lower boundaries of the cortical bone accurately. This task requires generation of two images, A and B, specified in sections 3.1 and 3.2. The images are inputs to a contour extraction method described in section 3.3, leading to determination of the desired boundaries. The algorithm is based on linear and morphological filtering.

The algorithm has been tested for images having fixed resolution. For other resolutions different mask sizes (M1 and M2, defined below) should be applied when low-pass and high-pass filtering an image.

3.1 Image A

Image A provides the upper boundary of the cortical bone. The algorithm consists of six steps; input image is the ROI cut:

- High-pass filtering (M1 mask),
- Low-pass filtering (M1 mask), twice,
- Image brightness normalization,
- Thresholding
- Selection of the biggest object.

3.1.1 High-pass and Low-pass Filtering

A signal can be treated as the sum of low-pass and high-pass components. Using this observation, high-pass filtering can be done as follows:

$$J = I - LOWPASS(I, M1), \qquad (1)$$

where I is the original image, LOWPASS(I,M1) means low-pass filtering of image I using mask M1. The M1 mask is the matrix of 31x31 elements equal to $1/31^2$, and has a notch filter characteristic.

Image J is low-pass filtered using the same mask M1, the operation is performed twice. It leads to boundary adjustment (less roughness), but some blurring, which is corrected in next steps. The use of a too small mask leads to important roughness of boundaries after thresholding operation. Of course, double low-pass filtering can be replaced by a single one at the expense of increased computational time.

3.1.2 Brightness Normalization

The next processing step relies on image brightness normalization. 5th and 95th percentiles of image histogram are computed and the L and H thresholds are obtained. Pixels are assigned an intensity of zero or one (maximum) if their brightness is below or above thresholds L and H respectively. If the pixel intensity is between L and H, a new pixel brightness score is assigned according to the equation

$$OUT(x, y) = \frac{1}{H - L} \cdot (IN(x, y) - L), \qquad (2)$$

where OUT is the output image, IN describes the input image, (x,y) are a pair of coordinates. This is a simple linear transformation which leads to contrast improvement in the interval <L,H>.

3.1.3 Thresholding

Only one global threshold is used, as experiments have shown good results have been obtained for threshold values T = 175/255 or T = 180/255. It should be emphasized that more accurate boundary determination is ensured for a variable threshold, but the algorithm is not fully automatic in such case.

Image thresholding based solely on highpass filtering (one global threshold) doesn't give good results, as artifacts tend to appear (many twigs). In such cases upper boundary extraction is difficult.

3.1.4 Selection of the Biggest Object

At this point the (binary) image contains many small structures, so the next step is to erase all objects but the one with the biggest surface (structures surfaces should be computed). An example is presented in figure 3. Upper part of its contour is the desired boundary to be extracted.

Figure 3: Example of image A.

3.2 Image B

Image B provides the lower boundary of the cortical bone. It is much better visible than the upper one, as the lower boundary occurs in the region of greater contrast. The algorithm consists of six steps:

- Opening (mask 5x5),
- Low-pass filtering (mask M2),
- High-pass filtering (mask M1),
- Image brightness normalization,
- Thresholding,
- Selection of the biggest object.

Initially the opening operation is carried out using a 5x5 window (all its elements equal to one), which involves two nonlinear filtering steps: a minimum filtering and a maximum filtering. A low-pass filtering mask M2 consists of 21x21 elements each having the value $1/21^2$. At this stage the image is blurred. High-pass filtering, which is the next step, emphasizes brightness differences and involves the use of the previously defined M1 mask. The image normalization stage has been described in section 3.1.2. Thresholding is performed using a global threshold T2 equal to 0.35, as a result a binary image is received. The biggest object is selected in the next step, its upper limit is the lower cortical bone boundary. A result is shown in figure 4.

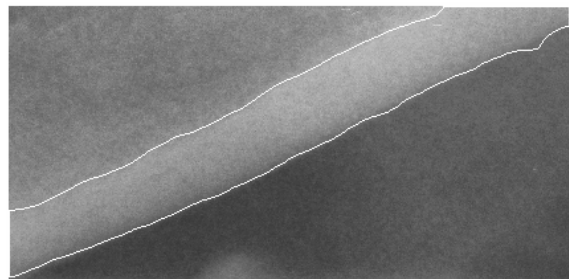Figure 4: Example of image B (same case as in figure 3).

Figure 5: Boundaries from Figures 3 and 4 superimposed on the original image.

3.3 Contour Extraction

The algorithm combines boundaries of images A and B. An exemplary result is shown in figure 5.

A and B images are inputs to the contour extraction method. RESULT is the result image, additionally, TEMP_TAB and POINTS tables are used, k and j are indices; at the beginning k and j equal one, while RESULT, TEMP_TAB contain zeros. The size of the RESULT image is the same and equal the size of the A image. The size of the TEMP_TAB equals the column number of the image A, the size of the POINTS table equals zero or one. LAST is the variable determing the number of column of image A.

1. Find the first white pixel in the k-th column in the image A (searching is done from the last row to the first one).
2. Find the first white pixel in the k-th column in the image B (searching is done from the first row to the last one).
3. If both pixels are found, execute the following tasks and go to step 7: join them by the shortest path (set of white pixels along the k-th column), mark the connection in the image A (put white pixel), TEMP_TAB[k]=1, check if the difference between TEMP_TAB[k] and TEMP_TAB[k-1] equals one, if it does, put current k value to the table POINTS.
4. If none of pixels is found, go to step 7.
5. If the white pixel from the image B is not found and the white pixel from image A is found, execute following tasks and go to the step 7: find the first white pixel in the k-th column of the image A (searching is done from the first row to the last row), remove all white pixels from column k (put black pixels), with the exception of the first white pixel found.
6. If the white pixel from the image B is found and the white pixel for the image A is not found, mark it in the A image (put white pixel) and continue (go to step 7).
7. k = k +1, if k≤LAST, go to step 1, otherwise continue.
8. Fill any holes in the image A.
9. Create RESULT image by extracting perimeter of image A (RESULT= PERIMETER(A)).
10. Find all indices {m} for which TEMP_TAB[m] – TEMP_TAB[m-1] equals -1, put them to the separate cells of the POINTS table, if the size of the POINTS table is greater than zero, go to the next step, otherwise stop the algorithm.
11. Find the first white pixels in the POINTS[j]-th column from the bottom and from the top of the image.
12. Assign zero values in the RESULT image to the pixels between pixels found (along the POINTS[j]-th column), j = j +1, if j is greater than the size of POINTS table, stop the algorithm, otherwise go to step 11.

The flowgraph of the contour extraction algorithm is shown in figure 6.

4 RESULTS

Forty images have been tested. The cortical bone contours were extracted. Thresholds T=175/255 and T=180/255 were used for the right and left side of the dental panoramic radiograph respectively (image A). The resulting boundaries have been presented to a radiologist for verification and have been either accepted or rejected. There is an irremovable element of subjectivity in such a test, boundaries sketched by a human aren't absolutely strict, and differ slightly from an evaluation session to another one.

Table 1: The upper boundary, the left side.

Clutter free (N=28)		Cluttered (N=12)	
Accepted	26	Accepted	4
Rejected	2	Rejected	8

Table 2: The lower boundary, the left side.

Clutter free (N=28)		Cluttered (N=12)	
Accepted	28	Accepted	8
Rejected	0	Rejected	4

Table 3: The upper boundary, the right side.

Clutter free (N=31)		Cluttered (N=9)	
Accepted	30	Accepted	4
Rejected	1	Rejected	5

Table 4: The lower boundary, the right side

Clutter free (N=31)		Cluttered (N=9)	
Accepted	31	Accepted	5
Rejected	0	Rejected	4

Tables 1, 2 and 3, 4 present verification results concerning the upper and lower cortical bone boundaries for the left and right side, respectively. Images have been classified either as cluttered or clutter free. The cluttered images contain structures which overlap the upper or lower cortical bone.

There have been 12 and 9 images in which other structures overlapped left or right side of DPR, respectively.

As can be seen, in the case of clutter-free images the results for extraction of cortical bone boundaries have been from very good (26 correct ones out of 28 possible for upper boundary, left side) to perfect ones (both lower boundaries). In contrast, results for cluttered images are rather poor. Note however that such images are easily discernible from the clutter-free ones. Moreover, whenever the method have failed, it has been very clear even for a non-specialist that the extracted boundaries did not define the cortical bone.

The particularly good results for the lower cortical bone extraction result from higher contrast at the edge of cortical bone. In the region of the upper boundary of cortical bone the contrast is usually much lower due to the presence of spongy bone. In some cases when positioning of the patient during x-ray examination was not performed correctly, the superimposition over the upper cortical boundary of other anatomical structures such as hyoid bone was observed in the form of "clutter". In a few cases the exact location of the upper cortical border was uncertain even to the radiologist due to factors mentioned above.

When comparing with existing methods (Devlin et al., 2007) note that the algorithm presented is neither complex nor a time consuming one. Firstly, in contrast to the method based on snakes it is non-iterative, results are obtained in a single run. Time complexity of each of its steps is O(n), i.e. the smallest possible. The prototype function written in MATLAB (version 7.0) realizing the algorithm executed in 0.4s for one image on 1.6 GHz Intel Celeron with 1GB RAM, an optimized program would be an order of magnitude faster. The snakes are moving across an image, the computation of a dislocation for each segment of a snake requires solving some equilibrium equations. Of course, it might be done quite time-effectively, if precision need not be high. Unfortunately, the method from (Devlin et al., 2007) forms a basis for a commercial software, hence, the details are not known.

When image contains structures that overlap the upper cortical bone, thresholding often do not lead to correct extraction. Note, however that unless a method has a human-like ability to draw a known shape on the basis of its small fraction, correct bone extraction in heavily cluttered images is a hopeless task. Straightforward use of snakes does not guarantee the success, too. That is why a clearly wrong outline of a cortical bone in such images seems to be a much better result than a shape that is probable, but highly imprecise one.

6 CONCLUSIONS

A new simple and effective algorithm for extracting cortical bone boundaries has been described in the paper. It consists of elementary operations available as functions in every image processing software package. The method works very well for clutter-free images, on the other hand, it is very clear when it fails in cases when the image is highly misleading. This combination of features is ideal for an untrained algorithm user, hence, the method is an excellent auxiliary tool for osteoporosis investigation by general dentist practitioners.

As it has been mentioned in the introduction, the proposed algorithm can be used for the cortical bone width determination, which seems to be useful for identification of women with low BMD level (Arifin A. et al., 2006). Future work will be concentrated on automatic cortical bone width measurement based on the proposed algorithm.

REFERENCES

Tosoni, G.M., Lurie, A.G., Cowan, A.E., Burleson, J.A., 2006. Pixel intensity and fractal analyses detecting osteoporosis in perimenopausal and postmenopausal women by using digital panoramic images. In *Oral Surgery, Oral Medicine, Oral Pathology, Oral Radiology, and Endodontics*. Vol. 102(2), pp. 235-241.

Horner K., Devlin H., Harvey L., 2002. Detecting patients with low skeletal bone mass. In *J. Dent.* Vol. 30, pp. 171-175.

Devlin H., Allen P.D., Graham J., Jacobs R., Karayianni K., Lindh C., van der Stel P.F., Harrison E., Adams J.E., Pavitt S., Horner K., 2007. Automated osteoporosis risk assessment by dentists: A new pathway to diagnosis. In *Bone*. Vol. 40, pp. 835–842.

Devlin C.V., Horner K., Devlin H., 2001. Variability in measurement of radiomorphometric indices by general dental practitioners. In *Dentomaxillofac Radiol*. Vol. 30, pp. 120-125.

Arifin A. Z.,Asano A., Taguchi A., Nakamoto T., Ohtsuka M., Truda M., Kudo Y., Tanimoto K., 2006. Computer-aided system for measuring the mandibular cortical width on dental panoramic radiographs in identifying postmenopausal women with low bone mineral density. In *Osteoporosis International*, Vol. 17, pp. 753–759.
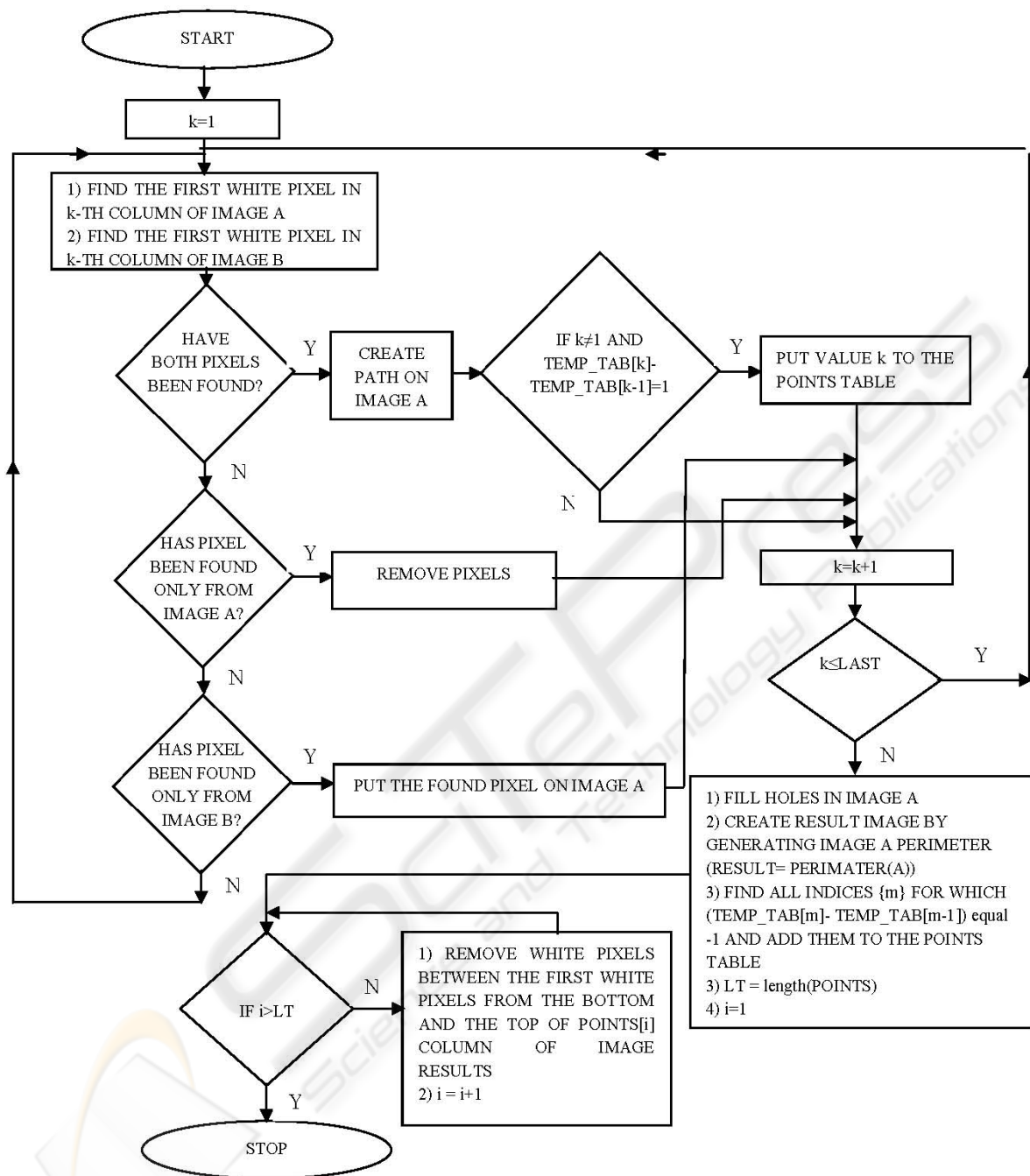
Figure 6: The flowchart of the contour extraction method.